Low-Field NMR Spectrometry of Chalk and Argillaceous Sandstones: Rock-Fluid Affinity Assessed from T_1/T_2 Ratio

Konstantina Katika[1], Milad Saidian[2], Manika Prasad[2], Ida L. Fabricius[1]

ABSTRACT

Nuclear magnetic resonance (NMR) procedure typically minimizes the effects of external magnetic field gradients on the transverse relaxation. Thus, longitudinal, T_1, and transverse, T_2, relaxation times should in principle be similar. However, internal magnetic field gradients related to minerals can shorten T_2, as compared to T_1, provided the saturating fluid has high affinity to the solid. Consequently, the T_1/T_2 ratio should quantify the affinity between the mineral and wetting pore fluid, so we estimate wettability from logging data by comparing the T_1/T_2 ratio of oil and water peaks in the reservoir zone to the T_1/T_2 ratio in the water zone. We tested the hypothesis on core samples and used the predicted wettability to successfully determining the elastic bulk modulus of samples containing oil and water.

In order to investigate the T_2-shortening, we performed 1D and 2D NMR experiments on samples of chalk, kaolinitic sandstone, and chloritic greensand, saturated either with water, oil or oil/water at irreducible water saturation. The 1D NMR experiment involved determination of T_2 spectrum, whereas the 2D NMR experiments included determination of T_1-T_2 and D-T_2 maps, where D is the intrinsic diffusion coefficient.

T_2 spectra show that in all water-saturated samples, surface relaxation dominates; in oil-saturated chalk and kaolinitic sandstone, bulk relaxation dominates; whereas T_2 of oil-saturated greensand shows surface relaxation in the part of the spectrum representing chlorite. In all samples with irreducible water saturation, water shows surface relaxation, whereas oil shows bulk relaxation. In line with this observation D-T_2 maps of these samples show field-gradient effects in the oil, but not in the water indicating that the water is trapped between solid and oil due to restricted diffusion.

A T_2 shortening will increase the T_1/T_2 ratio, so we use the T_1/T_2 ratio obtained from T_1-T_2 maps as a measure of fluid-mineral affinity. By this measure, the chalk shows high affinity for water, the kaolinitic sandstone has no clear preference for oil or water, whereas chloritic greensand shows different behavior for small and large pores. Small pores (fast-relaxing components) have $T_1/T_2 = 2.0$ when water saturated, but $T_1/T_2 = 3.8$ when oil saturated, indicating oil-affinity of chlorite. By contrast, large pores (slow-relaxing components) have significant preference for water ($T_1/T_2 = 2.2$) as compared to oil ($T_1/T_2 = 1.2$ to 1.4).

Overall, this paper provides an insight into the preference of a mineral to a fluid and ultimately into determining the wettability and correct pore-fluid distribution of a reservoir rock.

INTRODUCTION

This paper presents a method for estimating wettability in partially saturated reservoir rocks based on T_1/T_2 data acquired from low-field NMR spectrometry (Valori et al., 2013). Elucidating the wettability of a hydrocarbon reservoir is one of the major challenges in reservoir evaluation. The wettability of reservoir rocks affects the distribution of oil and water and the residual saturations of reservoir fluids. In a log interpretation context, elasticity data can be interpreted by Gassmann's (1951) fluid substitution if the fluid distribution in the pore space is known. When both oil and water are present in the pore space of a rock, the fluid wetting the surface of the mineral is expected to define the fluid supporting the solid frame and therefore dominates the fluid stiffness. In an oil-wet rock the bulk modulus of the oil is expected to dominate the elasticity of the fluid, whereas in a water-wet system the bulk modulus of the water is expected to dominate the elasticity of the pore fluid. Therefore, given the elasticity of a rock saturated with fluids of known elasticity, we determine the elasticity of the fluid mixture, and as a result, the fluid supporting the solid frame.

METHOD

The method requires two sets of T_1 and T_2 data: (1) at 100% saturation with a wetting fluid, and (2) at partial saturation with a wetting and a nonwetting fluid. NMR surface relaxation involves an adsorption of the pore fluid molecules at a short distance from the mineral surface, so only a wetting fluid will contribute to the surface relaxation (Howard, 1998). During the adsorption of molecules to the mineral, the close proximity of the mineral causes an increased relaxation of the T_2 signal relative to the T_1 signal, so a higher value of T_1/T_2 indicates that adsorption has taken place, and thus T_1/T_2 should be an indicator of wettability. In order to test the idea, we compare the T_1 and T_2 signals of three sets of plug samples, representing one chalk locality and two sandstone localities with variable mineralogy. Each set comprises three samples saturated respectively with water, oil, and with oil/water at irreducible water saturation.

Field Gradients

Low-field NMR spectrometry of porous media involves the measurement of the relaxation rate of the protons present in the pore fluid of a fully saturated medium (Dunn et al., 2002). Longitudinal and transverse relaxation representing fluid in a porous medium may both contain an element of bulk-fluid relaxation when the interaction of the fluid with the solid is small, but they are typically dominated by surface relaxation. In such case, molecular diffusion and limited pore size cause the majority of molecules to take part in solid-fluid interaction (Borgia et al., 1991; Kleinberg et al., 1993). In a uniform magnetic field, bulk and surface relaxation of low-viscosity fluids, such as brines and light oils, longitudinal and transverse relaxations are equal, but in the presence of external or internal magnetic field gradients a third relaxation mechanism is caused by the molecular diffusion. This mechanism affects the transverse relaxation (Dunn et al., 2002). External field gradients are due to the experimental setup, whereas internal field gradients are caused by the magnetic-susceptibility contrast between the fluid and the surface of the mineral, and may be enhanced by the presence of paramagnetic minerals (Dunn et al., 2002). The internal field gradients have short range and typically only affect the protons in fluids wetting the mineral surface. Therefore, given a magnetic-susceptibility contrast between the solid and the fluid, a direct physical adsorption of the fluid onto the solid is required to measure the surface relaxation (Le Doussal and Sen, 1992). The internal field gradients are difficult to predict precisely, but can be measured experimentally (Sun and Dunn, 2002). During NMR experiments, contributions due to internal or external field gradients are practically eliminated from the

longitudinal relaxation by using the inversion-recovery-free-induction-decay (IRFID) pulse sequence (Dunn et al., 2002). The contribution of the external field gradients can also be minimized when transverse-relaxation measurements are performed with the use of a CPMG (Carr-Purcell-Meiboom-Gill, named after the authors) pulse sequence (Dunn et al., 2002) at low Larmor frequencies but the effects of internal field gradients are not eliminated (Kleinberg et al., 1993). The experimental procedure can also be set up to enhance the effect of diffusion in an external field gradient, so the resulting intrinsic diffusion coefficient (D) can be used to discriminate between different pore fluids, and a 2D map of D versus T_2 can reveal the presence of internal field gradients (Hurlimann et al., 2003; Flaum et al., 2005; Zielinski et al., 2010).

T_1 and T_2

After each NMR relaxation measurement, an inversion technique converts the longitudinal and transverse relaxation decay curve into a T_1 and a T_2 spectrum, respectively (Dunn et al., 2002). Assuming that the bulk-fluid relaxation is slow compared to surface relaxation and that the relaxation due to field gradients is negligible, the longitudinal or transverse relaxation rates are similar, $1/T_{1,2}$, (1/s) and proportional to the surface-to-volume ratio, S/V, (1/μm) of the pore space:

$$\frac{1}{T_{1,2}} = \rho_{1,2} \frac{S}{V} \ . \tag{1}$$

The surface relaxivity, $\rho_{1,2}$, quantifies the ability of a mineral to enhance longitudinal and transverse relaxation, respectively, and is considered to be constant for any given solid-fluid system (Keating and Knight, 2012).

Several authors claim that T_1 or T_2 may be used to define the wettability of a formation (Hsu et al., 1992; Howard, 1998; Zhang et al., 2000; Guan et al., 2002; Heaton et al., 2002; Al-Mahrooqi et al., 2003; Fleury and Deflandre, 2003; Looyestijn and Hofman, 2006), but in most of these studies, rocks were saturated with a single fluid; either water or oil. When comparing different rocks with similar fluid, the observed relaxation rates are proportional to S/V. As a result, T_1 and T_2 measurements cannot be readily used to compare fluid-solid interactions of materials with different pore size. When using NMR logging data from hydrocarbon reservoirs, where both oil and water are present, a major limitation of using 1D T_1 or T_2 measurements for wettability determinations is that in complex pore systems oil and water cannot be separated from T_1 or T_2 alone since the water signal may overlap with the oil signal. In this case, the difference in the self-diffusion coefficient of each fluid, D, might in principle separate the signal of water and oil (Flaum et al., 2005). However, for $T_2 < 10$ ms, D is not measurable because

of hardware limitations (Jiang et al., 2013).

The interaction of fluids with a specific type of solid is reflected in the T_1/T_2 ratio because the ratio of relaxation times, T_1/T_2, is independent of pore geometry and is only affected by changes in the surface relaxivity. This is relevant when determining the surface and bulk relaxation of pore fluids, and the relaxation due to diffusion is negligible. For this reason, several authors used the T_1/T_2 ratio to study adsorption and desorption phenomena in porous catalysts (Weber et al., 2009; Mitchell et al., 2013; D'Agostino et al., 2014), and McDonald et al. (2005) used the T_1/T_2 ratio to describe the chemical exchange between water and cement paste. The T_1/T_2 ratio can be determined from 1D T_1 and T_2 measurements (e.g., Kleinberg et al., 1993), as well as from 2D NMR measurements, i.e., T_1-T_2 maps (e.g., Schoenfelder et al., 2008).

Samples and Procedures

The rock samples comprise three plugs of chalk, three plugs of kaolinite bearing sandstone and three plugs of chlorite-bearing greensand. The chalk is from Tor Formation of the Gorm field in the North Sea (Bæk, 2014), the kaolinite-bearing sandstone is from a quarry in the Berea Formation (Churcher et al., 1991) and the chlorite-bearing greensand is from the Solsort field in the North Sea (Bæk, 2014).

All samples are vertical and have the same size (37-mm diameter and 30-mm length). The plugs are divided into batches of three. Each batch comprises one plug of chalk, one greensand and one Berea sandstone plug. Core plugs were cleaned with the Soxhlet extraction technique, using methanol and toluene, and dried afterwards at 60°C for three days.

Characterization

Backscatter electron micrographs (BSEM) were recorded with a Quanta 200 (FEI) scanning electron microscope on polished thin sections of all samples. The mineral composition of all rocks and insoluble residues was identified by X-ray diffraction (XRD) by using Cu K-α radiation with a Philips PW 1830 diffractometer.

Specific Surface Area

The specific surface area (S_{BET}) of the samples with respect to weight (m²/g) was obtained with the nitrogen adsorption method using the Autosorb iQ gas sorption system from Quantachrome Instruments. Brunauer, Emmet and Teller (BET) inversion (Brunauer et al., 1938) was used to calculate the S_{BET} (multipoint).

Mercury Intrusion Capillary Curves

The MICP pore-throat-size distribution of the rocks was obtained with a Poremaster® PM 33-GT-12, mercury porosimetry analyzer and the conversion of pressure data to pore-throat-size distribution was performed with the Poremaster software from Quantachrome™ Instruments.

Porosity and Permeability Measurements

Helium porosity and Klinkenberg-corrected permeability were measured on cleaned and dried core plugs using a PoroPerm Production 2 gas porosimeter from Vinci Technologies. The bulk volume of the samples was determined from mercury immersion and Archimedes' principle.

Saturation

The first batch of core plugs was saturated only with salt water, the second batch only with dead oil and the third batch with dead oil and salt water at irreducible water saturation. The salt water was chosen to be 30,000 ppm NaCl solution and the selected dead oil came from the South Arne field, Danish North Sea (Bæk, 2014). The density of the salt water (1.019 g/cm³) and of dead oil (0.845 g/cm³) was measured using a digital density meter of high accuracy (±0.001). The dead oil properties are given in Table 1.

Table 1—South Arne Dead Oil Properties

Property	Crude oil
Density (g/cm³)	0.854
Viscosity (cP)	4.96
Total acid number (mg/g)	0.372
Total base number (mg/g)	2.076

For obtaining full water and oil saturation, Batches 1 and 2, pressure saturation was used. For the case of irreducible water saturation, Batch 3 was firstly fully saturated with salt water. For the chalk sample, oil was then flushed into the pore space until no more water is expelled from the rock. In order to achieve irreducible water saturation for Berea sandstone and greensand, porous-plate desaturation was used (Gray et al., 1993). All samples were kept 12 hours in a pressure vessel at 1,600 psi fully covered with oil in order to ensure full saturation. Complete saturation was verified by using the dry and saturated weight, grain volume by helium expansion, water and oil density. Information about the saturation is presented in Table 2. All samples were stored at ambient temperature and pressure for three months before the NMR measurements were performed.

Table 2—Saturation of the Core Plugs

Sample ID	Lithology	Batch	Water Saturation (%)	Oil Saturation (%)	Total Saturation (%)
N-3X-T1		1	100	0	100
N-3X-T2	Reservoir chalk	2	0	98	98
N-3X-T3		3	40	60	100
BS-T1		1	96	0	96
BS-T2	Berea sandstone	2	0	97	97
BS-T3		3	17	83	100
GSD-T1		1	100	0	100
GSD-T2	Reservoir greensand	2	0	100	100
GSD-T3		3	46	54	100

Batch 1 consists of the water-saturated rocks
Batch 2 consists of the oil-saturated rocks
Batch 3 consists of the water- and oil-saturated rocks at irreducible water saturation

T_2 Distributions

In the present study, the NMR measurements were made with a 2-MHz Magritek Rock Core Analyzer™ at 40ºC. T_2 relaxations were measured using the CPMG pulse sequence (Dunn et al., 2002) at a signal-to-noise ratio (SNR) equal to 250. The polarization time was selected at 5 s, the number of echoes at 16,000, and the echo spacing (TE) at 100 µs.

T_1- T_2 and T_2-D Measurements

T_1-T_2 and D-T_2 maps were constructed using similar acquisition parameters as in T_2 measurements for the transverse relaxation time (Sun et al., 2004). T_1 was measured using IRFID pulse sequence (Dunn et al., 2002). T_1 measurements were performed using 30 logarithmically spaced wait times ranging from 0.1 to 10,000 ms. A combination of CPMG and pulse-gradient-spin-echo (PGSE) experiments were used for T_2-D correlations (Latour et al., 1993). A pair of gradient pulses of duration, δ, 1.5 ms and separation, Δ, of 10 ms, was applied on both sides of the 180° pulse. The strength, g, of the gradient pulses was incremented between experiments. We used 16,000 echoes and TE at 100 µs. The raw 2D data were analyzed using 2D distribution function and an inverse Laplace transform to generate the 2D maps (Venkataramanan et al., 2002; Hürlimann et al., 2003; Song, 2010). For pure fluids, the fluid diffusivity was measured with the PGSE pulse sequence prior to the experiments (Latour et al., 1993).

Elastic-Wave Measurements

Elastic-wave velocities were measured, before and after the saturation, by placing the sample between two pistons of a loading frame under uniaxial unconfined compression at 2 MPa. The compressional- and shear-wave velocity were measured by recording the travel time of a transmitted ultrasonic wave at 200 kHz through the sample.

In order to evaluate the stiffness of the rock we calculated the elastic moduli that are related to the dynamic properties of the rock. The compressional-wave modulus, M (GPa), is related to the compressional-wave velocity, V_P (km/s), and the density, P (g/cm³). The shear-wave modulus, G (GPa), is related to the shear-wave velocity, V_S (km/s), and the density. The two moduli provide information about the bulk modulus, K (GPa), of the rock as shown in the following equations:

$$M = PV_P^2 \tag{2}$$

$$G = PV_S^2 \tag{3}$$

$$K = PV_P^2 - \frac{4}{3}PV_S^2. \tag{4}$$

The drained bulk modulus, K_f (GPa) was also modeled from Gassmann's fluid substitution, for all the fluid-saturated rocks (Gassmann, 1951):

$$\frac{K_{sat}}{K_m - K_{sat}} = \frac{K_f}{K_m - K_f} + \frac{K_{fl}}{\phi(K_m - K_{fl})}, \tag{5}$$

where K_{sat} is the bulk modulus for the saturated rock, ϕ is the porosity, K_m is the mineral bulk modulus and K_{fl} is the modulus of the saturating fluid. The effective mineral bulk modulus for greensand was estimated using the Voigt-Reuss-Hill average (Mavko et al., 2009) (Fig. 1). The bulk modulus of the fluids, were determined from Batzle and Wang (1992). The modulus of each mineral and fluid used in our modeling are given in Table 3. For comparison, the bulk modulus of the two-fluid-solid system was determined in two ways; in the softest (Reuss, 1929) and the stiffest way (Voigt, 1910).
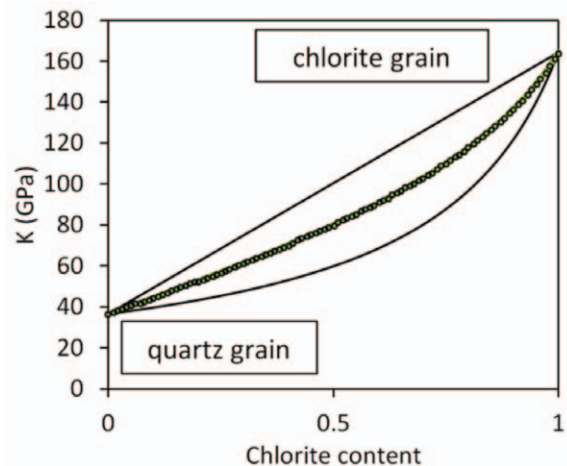

Fig. 1—Solid-grain bulk modulus of quartz-chlorite mixtures as a function of chlorite fraction. The outer two curves represent the Voigt and Reuss bounds (citation in Mavko et al., 2009). The dotted curve in the middle is calculated from Hill's average (Hill, 1952).

Table 3—Bulk and Shear Moduli of the Minerals and Fluids

Mineral/Fluid	K (GPa)	G (GPa)
Calcite	70	29
Quartz	36.6	45
Quartz and chlorite mixture	50	45
Salt water	2.32	-
Crude oil	1.6	-

Data are based on citations in Mavko et al. (2009)

RESULTS

Characterization

Backscatter electron micrographs of all lithologies are shown in Fig. 2. The mineral composition of all rocks is given in Table 4. The chalk has a bimodal grain-size distribution, but the pore space is homogeneous. The Berea sandstone is rich in quartz and part of the pore space contains loose kaolinite. The greensand is rich in quartz and chlorite grains as well as pore-filling chlorite. The specific surface area of the samples with respect to weight (m^2/g), helium porosity, and Klinkenberg corrected permeability for all samples is given in Table 5. The pore-throat-size distribution of all rocks is given in Fig. 3.

Table 4—Mineral Composition of the Core Material

Mineral	Reservoir Chalk	Berea Sandstone	Reservoir Greensand
Quartz	m	M	M
K-Feldspar	m	m	traces
Calcite	M	-	traces
Kaolinite	m	M	m
Chlorite	m	m	M
Illite	-	m	m

M - Represents the major components from XRD analysis
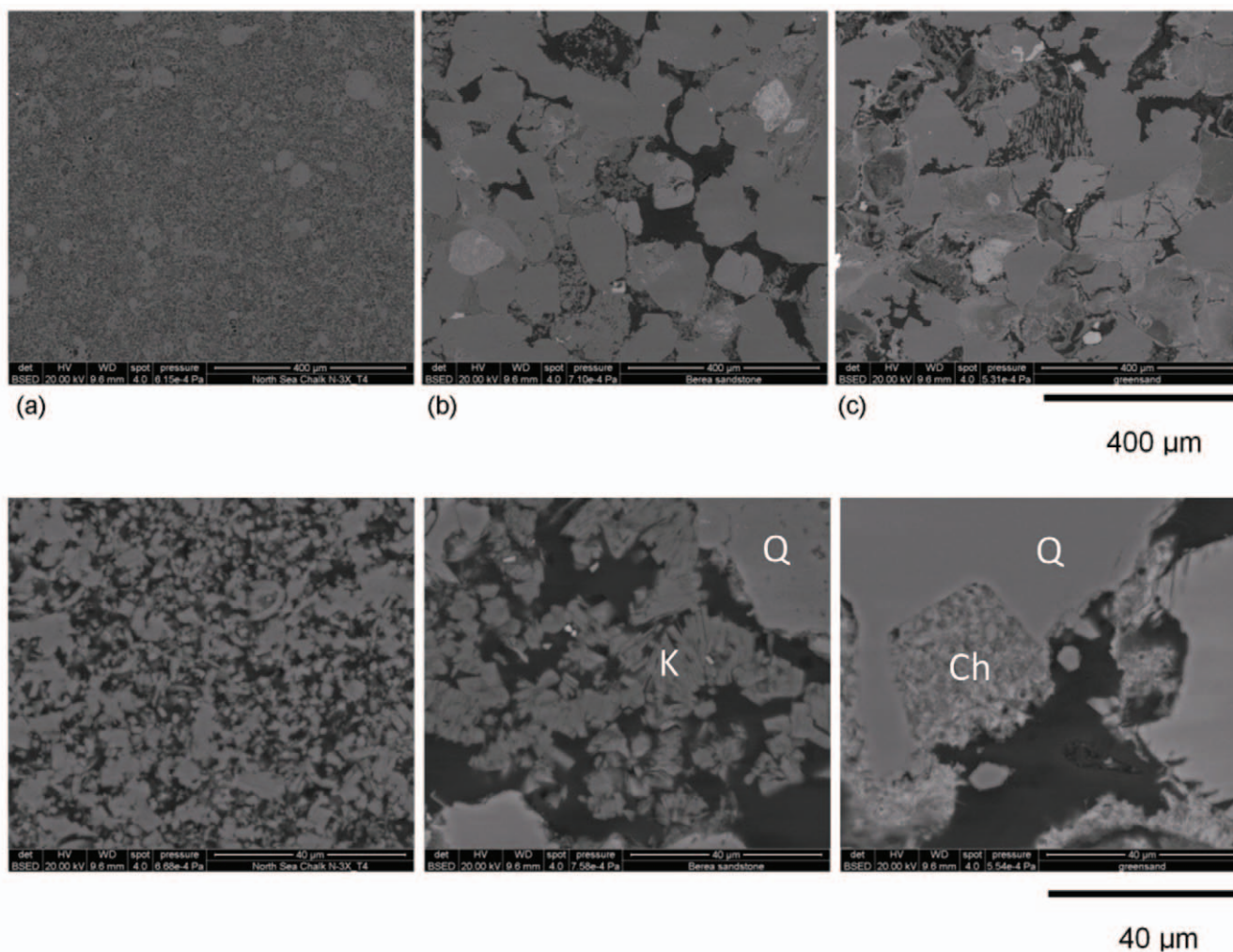m - Represents the minor components from XRD analysis

Fig. 2—Low- (top row) and high-resolution (bottom row) backscatter electron micrographs (BSEM) of the (a) reservoir chalk, (b) Berea sandstone, and (c) reservoir greensand. Black areas constitute pore space. "Ch" stands for chloride, "Q" for quartz and "K" for kaolinite.

Table 5—Petrophysical Properties of the Core Plugs

Sample ID	Grain Density (g/cm³)	Helium Porosity (fraction)	Klinkenberg Permeability (mD)	S$_{BET}$ (m²/g)	NMR-T_2 Porosity (fraction)
N-3X-T1	2.70	0.35	4.16	1.4	0.36
N-3X-T2	2.70	0.35	4.16	1.4	0.36
N-3X-T3	2.70	0.34	6.07	1.2	0.35
BS-T1	2.67	0.20	99.7	1.3	0.20
BS-T2	2.66	0.20	85.4	1.3	0.20
BS-T3	2.66	0.22	196.5	1.2	0.22
GSD-T1	2.73	0.32	117.6	8.7	0.32
GSD-T2	2.72	0.32	116.1	8.7	0.32
GSD-T3	2.73	0.32	111.4	8.7	0.33
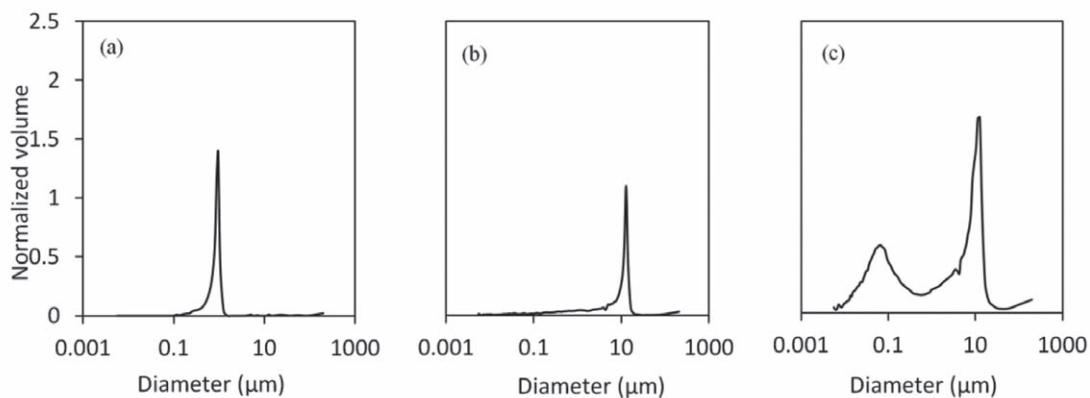
Fig. 3—The pore-throat-size distribution measured by mercury intrusion for (a) reservoir chalk, (b) Berea sandstone, and (c) reservoir greensand.

T_2 Measurements

The T_2 distributions of the bulk water (T_{2max} = 2,600 ms) and oil (T_{2max} = 470 ms) are shown in Figs. 4a and 4b, respectively. The crude oil is a mixture of different hydrocarbons that relax at different rates; hence, the broad T_2 spectrum (Rueslåtten et al., 1994; Flaum et al., 2005) (Fig. 4b). Figure 5 presents the T_2 distributions for each lithology for each saturation state. The T_{2max} values (highest peaks of the distribution) are shown in Table 6. The NMR porosity of the fully water-saturated plugs was derived from the T_2 distributions of the water-saturated core plugs (first column in Fig. 5) according to Coates et al. (1999) and given in Table 5.
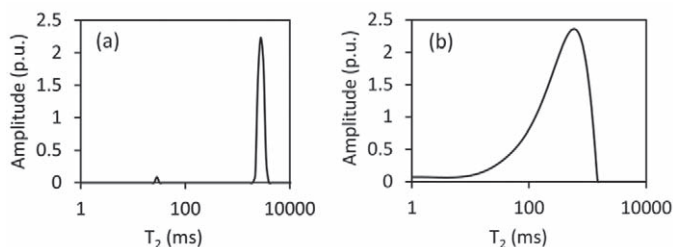
Fig. 4—The T_2 distribution of the (a) bulk water and (b) bulk oil.

T_1/T_2 Ratio from T_1-T_2 Maps

Figure 6 presents the T_1-T_2 maps. We divided each T_1-T_2 map in two regions: one for relaxation times < 50 ms and the other for higher values. For each region, the T_1/T_2 ratio was calculated at the point of highest intensity in the map, $(T_1/T_2)_{max}$ (light yellow color). The $(T_1/T_2)_{LM}$ values for the same regions were also determined from the logarithmic mean value of the projections of the two distributions. For example, in the case of water-saturated chalk we only observe one region for T_1/T_2 ratio > 50 ms, whereas, when the same rock contains oil and water, two regions are seen in the same map. Table 6 summarizes all the results.

D-T_2 maps

Figure 7 presents the D-T_2 maps for all the plugs where lines have been drawn that illustrate the D-T_2 correlation of the bulk water and oil (Hurlimann et al., 2003). The horizontal line in each map indicates the molecular diffusion coefficient of water (2.58×10^{-10} m²/s at 40°C); the inclined line indicates the diffusion-relaxation correlation for the crude oil used in this study based on the molecular diffusion coefficient of the oil (2.42×10^{-9} m²/s at 40°C) as well as the density and viscosity in Table 1 (Lo et al., 2002).
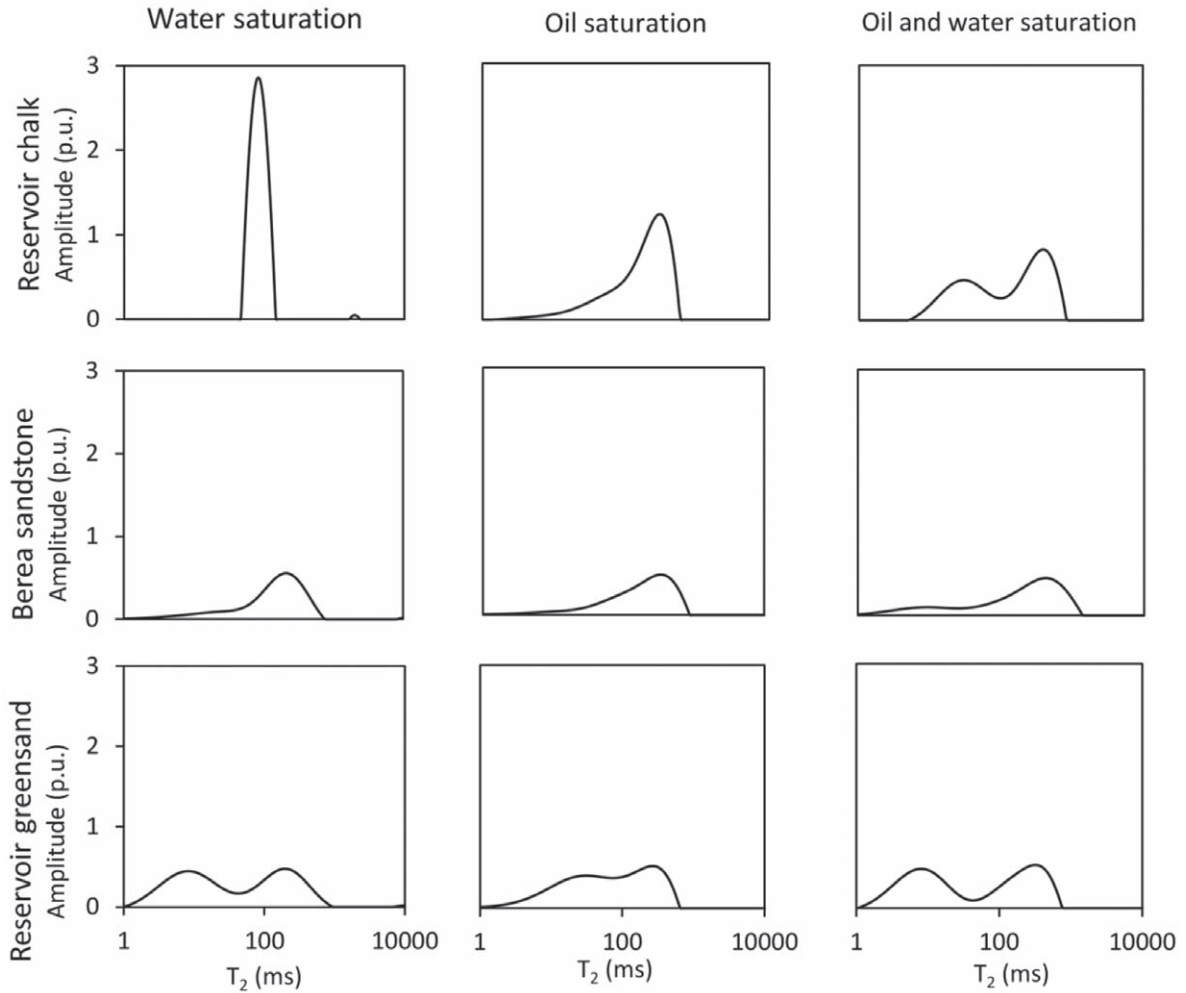
Fig. 5—The T_2 distributions of the reservoir chalk (top row), Berea sandstone (middle row) and reservoir greensand (bottom row). The left column represents rocks saturated with water, the center column rocks saturated with oil and the right column rocks saturated with oil and water at irreducible water saturation.

Table 6—The T_{2max} Values from Fig. 5, $(T_1/T_2)_{max}$ and $(T_1/T_2)_{LM}$ Ratio of the Rocks from the T_1-T_2 2D Maps in Fig. 6

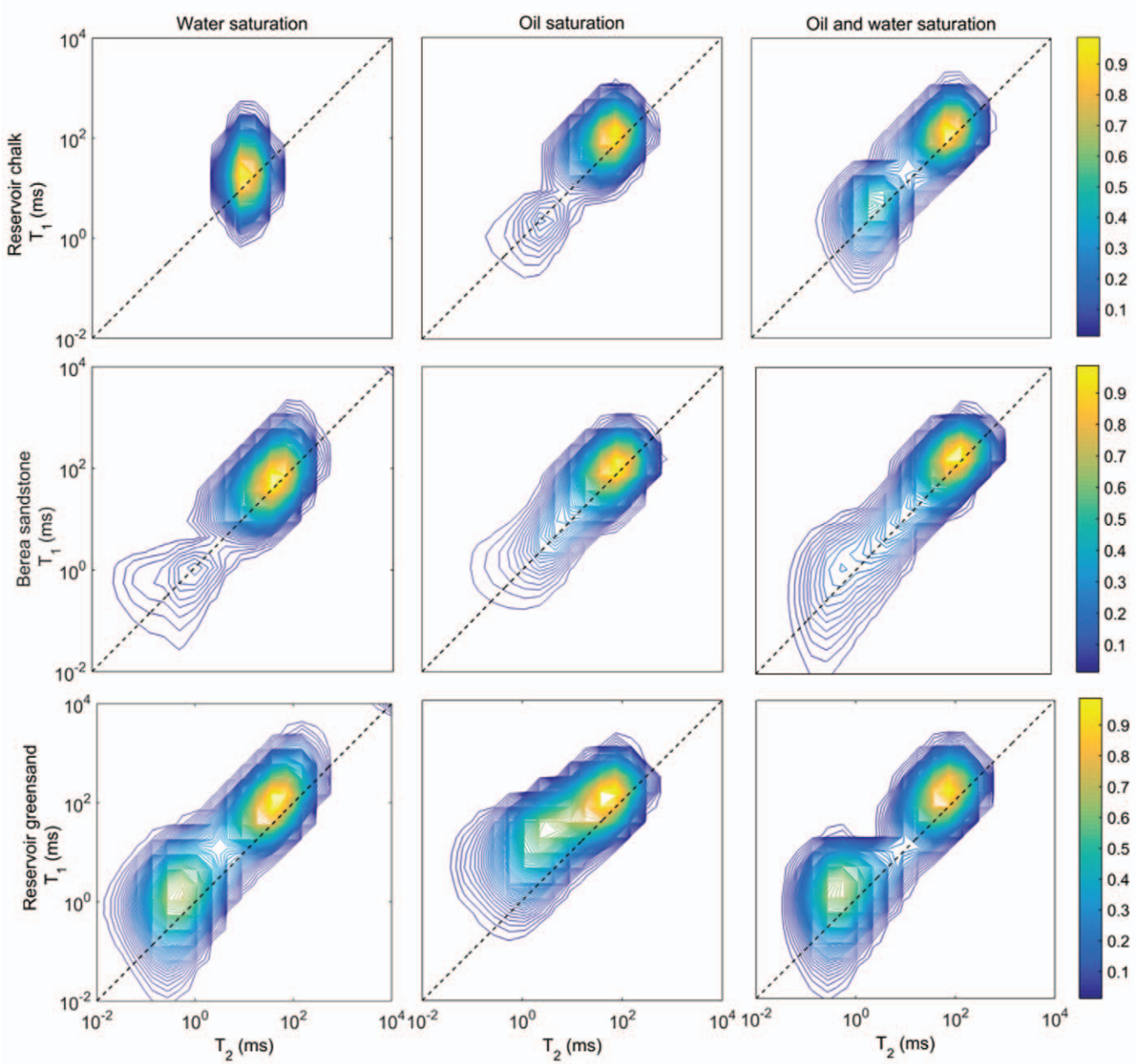| Sample	$T_{1,2}$ < 50 ms T_{2max} (ms)	$T_{1,2}$ > 50 ms T_{2max} (ms)	$T_{1,2}$ < 50 ms $(T_1/T_2)_{LM}$	$T_{1,2}$ > 50 ms $(T_1/T_2)_{LM}$	$T_{1,2}$ < 50 ms $(T_1/T_2)_{max}$	$T_{1,2}$ > 50 ms $(T_1/T_2)_{max}$
N-3X T1	-	82	-	1.8	-	2.0
N-3X T2	38	293	1.0	1.1	1.0	1.2
N-3X T3	29	391	1.9	1.0	2.3	1.4
BS-T1	-	195	-	1.1	-	1.2
BS-T2	9.7	348	1.0	1.2	1.1	1.1
BS-T3	9.6	415	1.0	1.2	1.4	1.1
GSD-T1	8.1	195	1.4	1.4	2.0	2.2
GSD-T2	30	366	2.2	1.0	3.8	1.2
GSD-T3	8.1	310	1.6	1.1	1.9	1.6

Fig. 6—T_1-T_2 maps of reservoir chalk, Berea sandstone and reservoir greensand. The left column represents rocks saturated with water, the center column represents rocks saturated with oil and the right column represents rocks saturated with oil and water at irreducible water saturation.
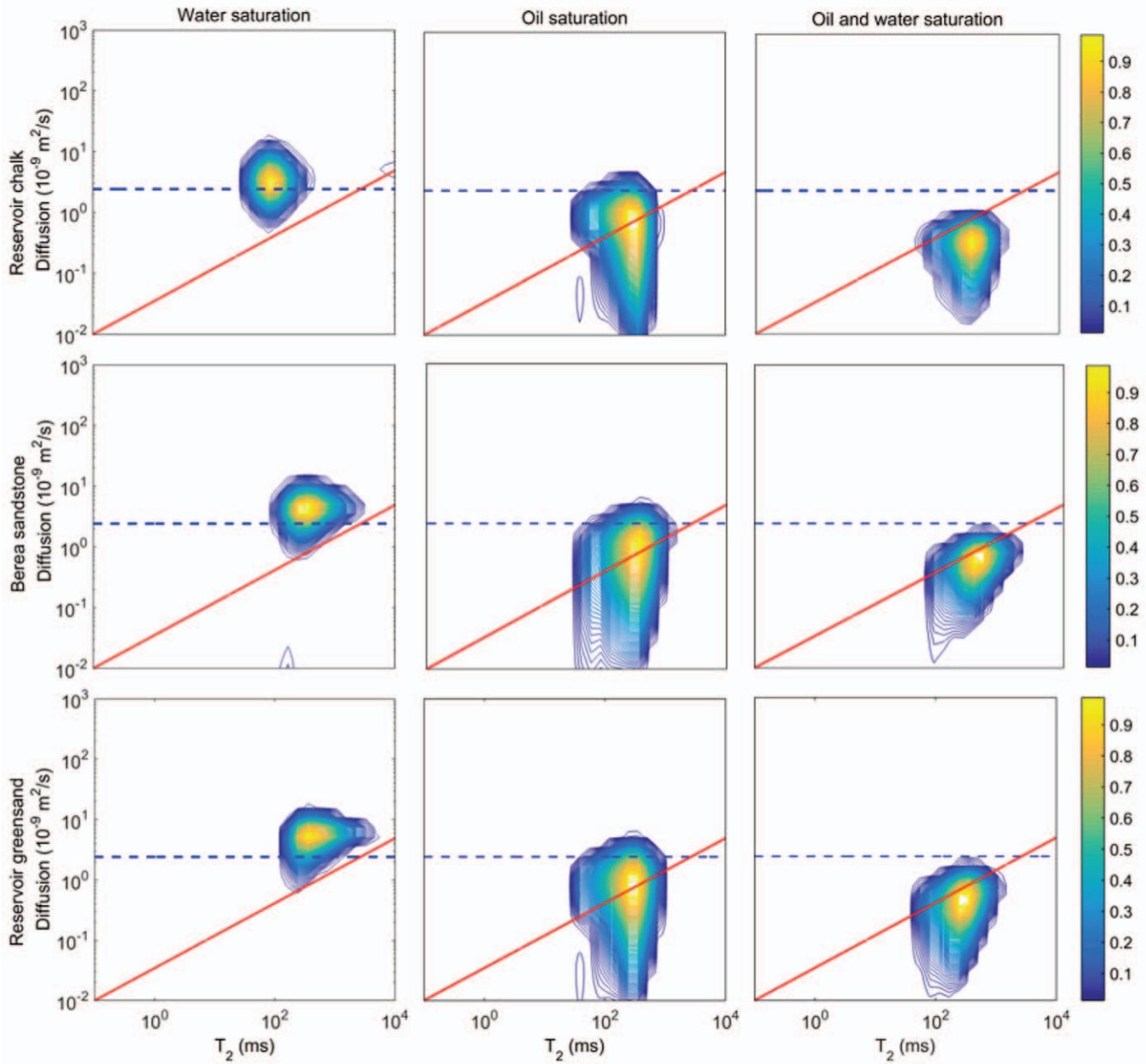
Fig. 7—The D-T_2 maps of reservoir chalk, Berea sandstone and reservoir greensand. The left column represents rocks saturated with water, the center column represents rocks saturated with oil and the right column represents rocks saturated with oil and water at irreducible water saturation. The horizontal dashed line indicates the molecular diffusion coefficient of water, whereas the inclined dashed line shows the correlation between the average diffusion coefficient and average relaxation times of oil according to Hurlimann et al. (2002).

Fluid Substitution

Figure 8a illustrates the K_f of the water-saturated rocks compared to the K_f of the rocks saturated with both oil and water where the effective bulk modulus of the mixed fluid was determined using the Voigt bound. Figure 8b illustrates the K_f of the oil-saturated rocks compared to the K_f of the

rocks saturated with both oil and water as the effective bulk modulus of the mixed fluid was determined using the Reuss bound. In both figures, all values of K_f were subtracted from the K_{dry} to minimize the visual effects of differences among the samples. All the bulk moduli reported in the present study are summarized in Table 7.
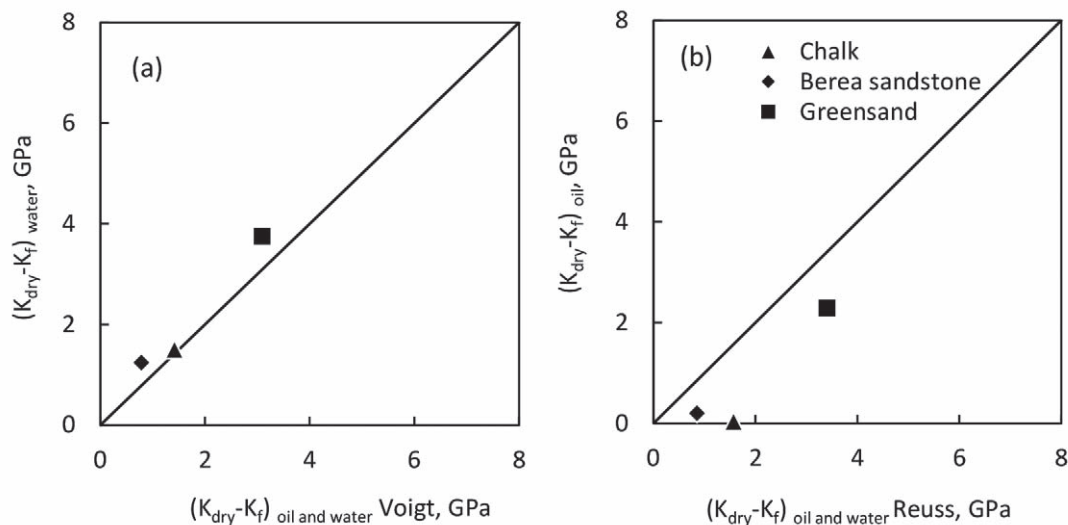
Fig. 8—(a) The frame bulk modulus, K_p, of the water-saturated rocks vs. the frame bulk modulus, K_p, of the oil- and water-saturated rocks at irreducible water saturation where the Voigt bound defines the effective bulk modulus of the fluids in the pore space. (b) The value of K_f of the oil-saturated rocks vs. the value of K_f of the oil- and water-saturated rocks at irreducible water saturation where the Reuss bound defines the effective bulk modulus of the fluids in the pore space. All values of K_f are subtracted from the K_{dry} value of the samples in order to focus on fluid effects.

Table 7—The Frame Bulk Modulus Defined by Gassmann's Fluid Substitution, K_p, of the Chalk, Berea Sandstone and Greensand

Bulk Modulus (GPa)	Reservoir Chalk	Berea Sandstone	Reservoir Greensand
K_{dry}	6.31	4.60	5.93
K_f of oil-saturated rocks	6.27	2.31	5.72
K_f of water-saturated rocks	5.85	2.64	12.86
K_f of oil- and water-saturated rocks at Reuss bound	5.69	2.33	12.79
K_f of oil- and water-saturated rocks at Voigt bound	5.06	2.23	12.39

DISCUSSION

Bulk and Surface Transverse Relaxation

The NMR porosity values are similar to the porosity measured with helium expansion on dry rocks (Table 5), and the T_2 distributions of the water-saturated chalk, Berea sandstone and greensand shown in Fig. 5 resemble the pore-throat-size distributions as obtained from the MICP measurements (Fig. 3). A similarity of the two distributions has been noted in several porous rocks, including Bentheimer sandstone, Berea sandstone and Texas Cream limestone (Marschall et al., 1995; Liaw et al., 1996). The slow bulk relaxation of the free water (Fig. 4a) seems to have no effect on the T_2 distribution of the water-saturated rock, indicating that the solid-fluid interaction dominates the transverse relaxation.

By contrast, the T_2 distribution of the oil-saturated chalk and Berea sandstone (center column in Fig. 5) resembles the

T_2 spectrum of the free oil (Fig. 4b) and does not reflect the pore-size distribution of each lithology given in Fig. 3. If the value of T_{2max} for the oil-saturated rocks, was used in Eq. 1, then the S/V, and as a result the pore diameter, would be underestimated, for a standard value of surface relaxivity. In such cases, the adsorption of the fluid to the mineral is significantly low, despite the fact that the magnetic susceptibility contrast between the oil and the mineral is high (Clark and Emerson, 1991). The bulk relaxation of the oil dominates the transverse relaxation and surface effects are not visible in the T_2 distribution from any fast-relaxing components; and Eq. 1 no longer describes the total relaxation. The T_{2max} of the free oil ($T_{2max} = 470$ ms) is similar to the oil-saturated rock for chalk and sandstone. Given the fact that the surface relaxation for chalk and sandstone is 82 and 195 ms, respectively (Fig. 5), this is an indication that the fluid, in this case the oil, has a minimum interaction with the solid. This observation is in accordance with previous

studies, which illustrate that the T_2 distribution is a reflection of the pore-size distribution only if the fluid wets the rock (Guan et al., 2002; Fleury and Deflandre, 2003). In Fig. 5, the T_2 distribution of the oil-saturated greensand reflects the bulk relaxation of the free oil (T_{2max} = 348 ms), and a solid-fluid interaction is also indicated since a second peak at lower relaxation times is present (T_{2max} = 30 ms). The T_2 spectrum of the oil-saturated greensand is thus the result of both surface and bulk relaxation in the pore space. It is worth mentioning that an investigation conducted on reservoir greensands from the North Sea, indicated that chlorite is preferably oil-wet (citation in Barclay and Worden, 2000; Lessenger et al., 2015).

The T_2 distribution of the oil- and water-saturated chalk, Berea sandstone and greensand has two peaks: the left peak probably is the result of solid-bound-water interaction, whereas the right peak resembles the bulk relaxation of the free oil. This observation is in accordance with Talabi and Blunt (2010) and Guan et al. (2002). The water interacts with the surface of the mineral while the oil relaxes according to the bulk relaxation suggesting that there is no interaction of this fluid with the pore walls.

Internal Field Gradients and Restricted Diffusion

The correlation of T_2 and self-diffusivity coefficient for the fluid in the pore space of the water-saturated chalk matches the water line (horizontal line in Fig. 7) of the map in the left column of Fig. 7. For the case of the water-saturated Berea sandstone and greensand, the D-T_2 correlation of the fluid in the rock shows a higher self-diffusivity coefficient than the water indicating the presence of internal field gradients (Hürlimann et al., 2004; Flaum et al., 2005).

The D-T_2 correlation of chalk, Berea sandstone and greensand fully saturated with oil matches the free-oil line at the highest intensity point (inclined line in Fig. 7). Effects of the internal field gradients are not expected in the oil-saturated chalk and Berea sandstone, since there is no oil-solid interaction. In the case of greensand the single peak indicates that effect of diffusion of oil is only seen for the large pores. Probably because the T_2 < 10 ms (as observed before in Fig. 5), of the short peak is shorter than the gradient separation (Δ = 10 ms) in the PGSE measurements. The first relaxing component should be "slower" than 10 ms in order to be recorded from the PGSE measurements.

For the rocks that have both oil and water in the pore space we might expect to see two different regions: one matching the water line and one matching the oil line due to the difference in the self-diffusion coefficient of the two fluids. The T_2 projections of the 2D maps of the oil and water-saturated chalk and sandstone include both oil and water relaxation rates and match the first and second graph

of the right column of Fig. 5. The short relaxation of the fast-relaxing components of greensand cannot be seen in the T_2 projection of the 2D maps of the oil and water-saturated rock in Fig. 5 due to the low values of the gradient separation. According to the projections of the axes of each 2D map in Fig. 7, the short-relaxing components are only visible in the x-axis, (where the T_2 is presented) but the diffusion was not properly measured in the y-axis due to the long gradient separation. Therefore, a correlation of these two values was not achieved and the final graph did not contain this information. But, in the 2D maps we observed only values below the horizontal "water" line indicating restricted diffusion. This is in accordance with previous studies that illustrated that the water is unable to illustrate the effects of the external field gradients unless the amount of water present in the rocks is high (Hürlimann et al., 2004; Flaum et al., 2005).

Wettability Determination from T_1/T_2

In the case of chalk, the T_1/T_2 ratio is higher when there is water instead of oil present in the pore space, when the values decrease from T_1/T_2 = 2 to 2.3 to T_1/T_2 = 1 to 1.4, respectively. In the case of both oil- and water-saturated chalk, the left peak has higher T_1/T_2, representing the strong attraction of the water to the surface (Fig. 6).

In the case of Berea sandstone the T_1/T_2 ratio varies between T_1/T_2 = 1 and 1.4, in both regions when there is either water or oil present in the pore space. In the case of both oil- and water-saturated rock, the first peak has relatively higher T_1/T_2, but the negligible differences could be interpreted as a neutral response to both water and oil.

In the case of greensand the T_1/T_2 ratio of the fast-relaxing components (small pores) is higher when there is oil (T_1/T_2 = 3.8) instead of water (T_1/T_2 = 2.0) present in the pore space. By contrast, the slow-relaxing components (big pores) have a higher ratio when in contact with water (T_1/T_2 = 2.2) than with oil (T_1/T_2 = 1.2). Of the two minerals that dominate the mineralogy of greensand, chlorite occupies the small pores and shows high oil attraction compared to quartz. This is an indication of the mixed wettability of the rock.

Fluid Distribution

From the bulk moduli of the oil- and water-saturated chalk illustrated in Fig. 8a we observe that the K_f calculated at the Voigt bound is similar to the K_f of the water-saturated chalk, and that using the Reuss bound for chalk leads to a huge overestimation of the frame stiffness (Fig. 8b). This indicates that for the case of chalk in the presence of both oil and water in the pore space, water is the fluid supporting the frame. For the two sandstones, using the Voigt bound

leads to lower frame stiffness (Fig. 8a) indicating that the fluid mixture is softer than the Voigt bound. On the other hand, using the Reuss bound leads to high prediction of the frame stiffness, indicating that the fluid mixtures are stiffer than the Reuss bound (Fig. 8a), so that a Hill average is recommendable. These observations support the results for NMR, indicating that the chalk is water-wet whereas the two sandstones are intermediate, respectively mixed-wet.

CONCLUSIONS

Low-field NMR and ultrasonic velocity measurements were done on reservoir chalk, Berea sandstone and chloritic greensand at three different saturation states; water, oil as well as oil and water at irreducible water saturation. The following approach to quantify the solid-fluid affinity and fluid distribution in a rock was used:

- The pore fluid of the reservoir rock relaxes as a free fluid or due to the solid-fluid interaction in the porous medium. Surface relaxation of a pore fluid indicates solid-fluid affinity, whereas bulk relaxation indicates the opposite.
- The T_1/T_2 ratio was used as an indicator to quantify the fluid-solid affinity in reservoir rocks. The T_1/T_2 ratio illustrates the strength with which a fluid adsorbs on a solid; the higher the adsorption strength the higher the ratio. The fluid wetting the surface of a mineral has a higher ratio than other fluids present in the pore space.
- The fluid distribution obtained from the T_1/T_2 ratio can be applied when estimating the fluid moduli in rocks, bearing two fluids. The compounds should be mixed according to the Voigt average in the water-wet case, the Reuss average in the oil-wet case and a Hill average in the intermediate or mixed-wet case. This is relevant for Gassmann's fluid substitution in elasticity studies for core and log analysis.

ACKNOWLEDGMENTS

NOMENCLATURE

Abbreviations

BET = Brunauer-Emmet-Teller

NMR = nuclear magnetic resonance
IRFID = inversion-recovery-free-induction-decay pulse sequence
CPMG = Carr-Purcell-Meiboom-Gill pulse sequence
MICP = Mercury intrusion capillary pressure curves
PGSE = Pulsed gradient spin-echo

Symbols

D = intrinsic diffusion coefficient
g = strength of the gradient pulses
G = shear-wave modulus
K = bulk modulus
K_f = bulk modulus of the drained rock
K_m = bulk modulus of the mineral
K_{fl} = Bulk modulus of the saturating fluid
K_{sat} = bulk modulus for the saturated rock
M = compressional-wave modulus
S_{BET} = specific surface area with respect to weight
S/V = surface-to-volume ratio
TE = echo spacing
T_1 = longitudinal relaxation time
T_2 = transverse relaxation time
T_{2max} = highest T_2 value of the distribution
V_P = compressional-wave velocity
V_S = shear-wave velocity
δ = duration of gradient pulses
Δ = separation time of gradient pulses
P = density
ρ = surface relaxivity
ϕ = porosity

REFERENCES

Al-Mahrooqi, S., Grattoni, C.A., Moss, A.K. and Jing, X.D., 2003, An Investigation of the Effect of Wettability on NMR Characteristics of Sandstone Rock and Fluid Systems, *Journal of Petroleum Science and Engineering*, **39**(3–4), 389–398. DOI: http://dx.doi.org/10.1016/S0920-4105(03)00077-9

Barclay, S.A., and Worden, R.H., 2000, Effects of Reservoir Wettability on Quartz Cementation in Oil Fields, *in* Worden, R.H., and Morad, S., Editors, *Quartz Cementation in Sandstones*, International Association of Sedimentologists, Special Publication **29**, Wiley-Blackwell Publishing Ltd., 103–117. ISBN: 9780632054824

Bæk, M., 2014, *Oil and Gas Production in Denmark 2013 and Subsoil Use*, Danish Energy Agency. ISBN: 978-87-93071-71-1. https://ens.dk/sites/ens.dk/files/OlieGas/oil_and_gas_in_denmark_2013.pdf. Accessed March 5, 2017.

Batzle, M.L., and Wang, Z., 1992, Seismic Properties of Pore Fluids, *Geophysics*, **57**(11), 1396–1408. DOI: 10.1190/1.1443207

Borgia, G.C., Fantazzini, P., and Messini, E., 1991, Wettability Effects on Oil-Water-Configurations in Porous Media: A

Nuclear Magnetic Resonance Relation Study, *Journal of Applied Physics*, **70**, 7623. DOI: http://doi.org/10.1063/1.349720

Brunauer, S., Emmett, P.H., and Teller, E., 1938, Adsorption of Gases in Multimolecular Layers, *Journal of the American Chemical Society*, **60**(2), 309–319. DOI: 10.1021/ja01269a023

Churcher, P.L., French, P.R., Shaw, J.C., and Schramm, L.L., 1991, Rock Properties of Berea Sandstone, Baker Dolomite, and Indiana Limestone, Paper SPE-21044 presented at the SPE International Symposium on Oilfield Chemistry, Anaheim, California, USA, 20–22 February. DOI: https://doi.org/10.2118/21044-MS

Clark D.A., and Emerson, D.W., 1991, Notes on Rock Magnetization Characteristics in Applied Geophysical Studies, *Exploration Geophysics*, **22**(3), 547–555. DOI: 10.1071/EG991547

Coates, G.R., Xiao, L., and Prammer, M.G., 1999, *NMR Logging Principles and Applications*: Halliburton Energy Services Publication H02308. http://www.halliburton.com/public/lp/contents/Books_and_Catalogs/web/NMR-Logging-Principles-and-Applications.pdf. Accessed March 6, 2017.

D'Agostino, C., Mitchell, J., Mantle, Michael D., and Gladden, L.F., 2014, Interpretation of NMR Relaxation as a Tool for Characterising the Adsorption Strength of Liquids inside Porous Materials, *Chemistry: A European Journal*, **20**(40), 13009–13015. DOI: 10.1002/chem.201403139

Le Doussal, P., and Sen P.N., 1992, Decay of Nuclear Magnetization by Diffusion in a Parabolic Magnetic Field: An Exactly Solvable Model, *Physical Review B*, **46**(6), 3465. DOI: https://doi.org/10.1103/PhysRevB.46.3465

Dunn, K.J., Bergman, D.J., and LaTorraca, G.A., 2002, *Nuclear Magnetic Resonance—Petrophysical and Logging Applications*, Handbook of Geophysical Exploration: Seismic Exploration, **32**, Elsevier Science. ISBN: 978-0444542533

Flaum, M., Chen, J., and Hirasaki, G. J., 2005, NMR Diffusion Editing for $D–T_2$ Maps: Application to Recognition of Wettability Change, *Petrophysics*, **46**(2), 113–123.

Fleury, M., and Deflandre, F., 2003, Quantitative Evaluation of Porous Media Wettability Using NMR Relaxometry, *Magnetic Resonance Imaging*, **21**(3–4), 385–387. DOI: http://dx.doi.org/10.1016/S0730-725X(03)00145-0

Gassmann, F., 1951, Uber die Elastizitaet poroeser Medien: Vierteljahresschrift der Naturforschenden Gesellschaft, Zuerich, **96**, 1–23.

Gray, R., Trewin, B., Pallatt, N., and Mitchell, P., 1993, Comparison of Saturation Exponent Data by the `Porous Plate' and by the `Continuous Injection' Technique with In Situ Saturation Monitoring, in Worthington, P.F., and Chardaire-Riviere, C., Editors, *Advances in Core Evaluation*, **3**, 293–316, Gordon and Breach Science Publishers. ISBN: 978-2881249044

Guan, H., Brougham, D., Sorbie, K.S., and Packer, K.J., 2002, Wettability Effects in a Sandstone Reservoir and Outcrop Cores from NMR Relaxation Time Distributions, *Journal of Petroleum Science and Engineering*, **34**(1–4), 35–54. DOI: http://dx.doi.org/10.1016/S0920-4105(02)00151-1

Heaton, N., Freedman, R, Karmonik, C., Taherian, R., Walter, K., and de Pavia, L., 2002, Applications of a New-Generation Wireline NMR Logging Tool, Paper SPE-77400 presented at the SPE Annual Technical Conference and Exhibition, San Antonio, Texas, USA, 29 September–2 October. DOI: https://doi.org/10.2118/77400-MS

Hill, R., 1952, The Elastic Behaviour of Crystalline Aggregate, *Proceedings of the Physical Society London*, **A65**(5), 349–354. DOI: 10.1088/0370-1298/65/5/307.

Howard, J., 1998, Quantitative Estimates of Porous Media Wettability from Proton NMR Measurements, *Magnetic Resonance Imaging*, **16**(5–6), 529–533. DOI: http://dx.doi.org/10.1016/S0730-725X(98)00060-5

Hsu, W., Li, X., and Flumerfelt, R.W., 1992, Wettability of Porous Media by NMR Relaxation Methods, Paper SPE-24761 presented at the SPE Annual Technical Conference and Exhibition, Washington, D.C., USA, 4–7 October. DOI: https://doi.org/10.2118/24761-MS

Hürlimann, M.D., Freedman, R., Venkataramanan, L., Flaum, C., Flaum, M., and Hirasaki, G.J., 2003, Diffusion-Relaxation Distribution Functions of Sedimentary Rocks in Different Saturation States, *Magnetic Resonance Imaging*, **21**(3–4), 305–310. DOI: http://dx.doi.org/10.1016/S0730-725X(03)00159-0

Hürlimann, M., Matteson, A., Massey, J.E., Allen, D.F., Fordham, E.J., Antonsen, F., and Rueslåtten, H.G., 2004, Application of NMR Diffusion Editing as Chlorite Indicator, *Petrophysics*, **45**(5), 414–421.

Jiang, T., Rylander, E., Singer, P.M., Lewis, R.E., and Sinclair, S.M., 2013, Integrated Petrophysical Interpretation of Eagle Ford Shale with 1-D and 2-D Nuclear Magnetic Resonance (NMR), Paper LL, *Transactions, SPWLA 54th Annual Logging Symposium*, New Orleans, Louisiana, USA, 22–26 June.

Keating, K., and Knight, R., 2012, The Effect of Spatial Variation in Surface Relaxivity on Nuclear Magnetic Resonance Relaxation Rates, *Geophysics*, **77**(5), E365–E377. DOI: 10.1190/geo2011-0462.1

Kleinberg, R.L., Farooqui, S.A., and Horsfield, M.A., 1993, T_1/T_2 Ratio and Frequency Dependence of NMR Relaxation in Porous Sedimentary Rocks, *Journal of Colloid Interface Science*, **158**(1), 195–198. DOI: http://dx.doi.org/10.1006/jcis.1993.1247

Latour, L.L., Li, L., and Sotak, C.H., 1993, Improved PFG Stimulated-Echo Method for the Measurement of Diffusion in Inhomogeneous Fields, *Journal of Magnetic Resonance*, Series B, **101**(1), 72–77. DOI: http://dx.doi.org/10.1006/jmrb.1993.1009

Lessenger, M., Merkel, D., Medina, R., Ramakrishna, S., Chen, S., Balliet, R., Xie, H., Bhattad, P., Carnerup, A., and Knackstedt, M., 2015, Subsurface Fluid Characterization Using Downhole and Core NMR T_1-T_2 Maps Combined with Pore-Scale Imaging Techniques, *Petrophysics*, **56**(4), 313–333.

Liaw, H.K., Kulkarni, R., Chen, S., and Watson, A.T., 1996, Characterization of Fluid Distributions in Porous Media by NMR Techniques, *AIChE Journal*, **42**(2), 538–546. DOI: 10.1002/aic.690420223

Lo, S.-W., Hirasaki, G.J., House, W.V., and Kobayashi, R., 2002, Mixing Rules and Correlations of NMR Relaxation Time with Viscosity, Diffusivity, and Gas/Oil Ratio of Methane/Hydrocarbon Mixtures, Paper SPE-77264, *SPE Journal*, **7**(1),

24–34. DOI: https://doi.org/10.2118/77264-PA

Looyestijn, W.J., and Hofman, J., 2006, Wettability-Index Determination by Nuclear Magnetic Resonance, Paper SPE-93624, *SPE Reservoir Evaluation & Engineering*, **9**(2), 146–153. DOI: https://doi.org/10.2118/93624-PA

Marschall, D., Gardner, J.S., Mardon, D., and Coates, G.R., 1995, Method for Correlating NMR Relaxometry and Mercury Injection Data, Paper SCA-9511 presented at the SCA International Symposium, San Francisco, California, USA, 12–14 September.

Mavko, G., Mukerji, T., and Dvorkin, J., 2009, *The Rock Physics Handbook: Tools for Seismic Analysis of Porous Media*, 2nd Edition, Cambridge University Press. ISBN 9780521861366.

McDonald, P.J., Korb, J.-P., Mitchell, J., and Monteilhet L., 2005, Surface Relaxation and Chemical Exchange in Hydrating Cement Pastes: A Two-Dimensional NMR Relaxation Study, *Physical Review E,* **72**(1), Paper 011409. DOI: https://doi.org/10.1103/PhysRevE.72.011409

Mitchell, J., Chandrasekera, T.C., Gladden, L.F., Broche, L.M., and Lurie, D.J., 2013, Exploring Surface Interactions in Catalysts Using Low-Field Nuclear Magnetic Resonance, *The Journal of Physical Chemistry C*, **117**(34), 17699–17706. DOI: 10.1021/jp405987m

Reuss, Z.A.A., 1929, Berechnung der Fliessgrenze von Mischkristallen auf grund der Plastizitätsbedingungen für Einkristalle: Zeitschrift für Angewandte Mathematik und Mechanik, **9**, 49–58.

Rueslåtten, H., Oren, P.E., Robin, M., and Rosenberg, E., 1994, A Combined Use of CRYO-SEM and NMR-Spectroscopy for Studying the Distribution of Oil and Brine in Sandstones, Paper SPE-27804 presented at the SPE/DOE Improved Oil Recovery Symposium, Tulsa, Oklahoma, USA, 17–20 April. DOI: https://doi.org/10.2118/27804-MS

Schoenfelder, W., Gläser H.R., Mitreiter I., and Stallmach, F., 2008, Two-Dimensional NMR Relaxometry Study of Pore Space Characteristics of Carbonate Rocks from a Permian Aquifer, *Journal of Applied Geophysics*, **65**(1), 21–29. DOI: http://dx.doi.org/10.1016/j.jappgeo.2008.03.005

Song, Y.Q., 2010, Recent Progress of Nuclear Magnetic Resonance Applications in Sandstones and Carbonates Rocks, *Vadose Zone Journal*, **9**(4), 828–834. DOI: 10.2136/vzj2009.0171

Sun, B., and Dunn, K.J., 2005, Two-Dimensional Nuclear Magnetic Resonance Petrophysics, *Magnetic Resonance Imaging*, **23**(2), 259–262. DOI: 10.1016/j.mri.2004.11.056

Sun, B., Dunn, K.J., Bilodeau, B.J., Van Dalen, S.C., Stonard, S.W., and Al-Rushaid, A., 2004, Two-Dimensional NMR Logging and Field Test Results, Paper KK, *Transactions, SPWLA 45th Annual Logging Symposium*, Noordwijk, The Netherlands, 6–9 June.

Talabi, O., and Blunt, M.J., 2010, Pore-Scale Network Simulation of NMR Response in Two-Phase Flow, *Journal of Petroleum Science and Engineering*, **72**(1–2), 1–9. DOI: http://dx.doi.org/10.1016/j.petrol.2010.01.013

Valori, A., Hürlimann, M.D., Nicot, B., and Bachman H.N., 2013, Obtaining Wettability From T_1 and T_2 Measurements, US Patent Application US2013325348 (A1), December 5, 2013.

Venkataramanan, L., Song, Y.Q., and Hürlimann, M.D., 2002, Solving Fredholm Integrals of the First Kind with Tensor Product Structure in 2 and 2.5 Dimensions, *IEEE Transactions on Signal Processing*, **50**(5), 1017–1026. DOI: 10.1109/78.995059

Voigt, W., 1910, Lehrbuch der Kristallphysik, Tuebner Verlag. A 1966 reprint is available from Springer. ISBN 978-3-663-15316-0.

Weber, D.W., Mitchell, J., McGregor, J., and Gladden, L.F., 2009, Comparing Strengths of Surface Interactions for Reactants and Solvents in Porous Catalysts Using Two-Dimensional NMR Relaxation Correlations, *The Journal of Physical Chemistry C*, **113**(16), 6610−6615. DOI: 10.1021/jp811246j

Zhang, Q., Huang, C., and Hirasaki, G., 2000, Interpretation of Wettability in Sandstones with NMR Analysis, *Petrophysics*, **41**(3), 223–233.

Zielinski, L., Ramamoorthy, R., Minh, C.C., Al Daghar, K.A., Sayed, R.H., and Abdelaal, A.F., 2010, Restricted Diffusion Effects in Saturation Estimates from 2D Diffusion-Relaxation NMR Maps, Paper SPE-134841 present at the SPE Annual Technical Conference and Exhibition, Florence, Italy, 19– 22 September. DOI: https://doi.org/10.2118/134841-MS

ABOUT THE AUTHORS

Konstantina Katika is a postdoctoral researcher in the Technical University of Denmark (DTU). Her current research focuses on petrophysics, geomechanics, rock physics, and solid-fluid interaction using low-field NMR spectrometry. She holds a PhD in rock physics from DTU, an MSc in geotechnical engineering from University of PATRAS (UPATRAS), and a MENg in Civil Engineering from UPATRAS. Konstantina may be contacted at koka@byg.dtu.dk.

Milad Saidian is a Petrophysicist at BP America Inc. in Houston, Texas. He has BSc and MSc in Petroleum Engineering from Petroleum University of Technology and Sharif University of Technology, respectively. He received his PhD from Colorado School of Mines in 2015. His interests include rock and fluid properties and pore space characterization using nuclear magnetic resonance and other techniques for conventional and unconventional reservoir rocks focusing on porosity and pore-size distribution measurement methods. Besides working at BP, his industrial work experience includes internships Maersk Oil Houston Inc., as petrophysicist; NIOC, as reservoir engineer; and Maroon Oil and Gas Production Company, as production field engineer.

Manika Prasad is a professor of Petroleum Engineering at the Colorado School of Mines. She directs the Center for Rock Abuse along with the OCLASSH (Organic, Clay, Sand, Shale) and DHI/Fluids (Direct Hydrocarbon Indicators) industry consortiums. Manika received a BS (Honors with distinction) in geology from Bombay University, an MS (Diplom) in geology with marine geology and geophysics as minors, and a PhD in geophysics, from the Christian-Albrechts-Universität at Kiel in Germany. Manika won the Merit Scholarship Award from the University of Bombay for her BS achievements and the Friedrich-Ebert-Stiftung Scholarship for PhD research at Kiel University. She has worked at the University of Hawaii, Stanford Rock Physics Laboratory at Stanford University, and at the Center for Rock Abuse at the Petroleum Engineering and Geophysics departments at Colorado School of Mines. She was Outstanding Mentor to Native American Students at Stanford during 2002–2003. Manika was the AAPG/SEG Distinguished Lecturer in Fall 2012 and was awarded the Outstanding Educator Award by SEG in 2015. Manika's main interests lie in understanding the basic principles governing the physical properties of rocks, fluids, and rocks with fluids. She is also interested in understanding how ant-sized phenomena control elephant-sized features. She has published widely in geophysical, geological, petroleum engineering, and nondestructive testing journals.

Ida Fabricius is a professor of Applied Geology at Technical University of Denmark (DTU). She received BSc degrees in chemistry and geography, as well as an MSc degree in geology from University of Copenhagen. She won the Copenhagen University gold medal for a dissertation on the geochemistry of sulfosalts of copper. After a few years as development geologist at Mærsk Oil, she joined DTU, where she completed her PhD and dr.techn. degrees on physical properties and diagenesis of chalk. Ida Fabricius has supervised more than hundred MSc thesis students and more than 20 PhD students, and is currently head of the Geotechnics and Geology Section of the DTU Civil Engineering Department. Her main research interest is integrating petrophysical, rock physical, rock mechanical and petrographic information.